Study of aluminized solid propellant fire at atmospheric pressure

Fabien Chassagne[1], Serge Bordachar[2], Hui Yin Wang[1] and Pierre Joulain[1]

[1]Laboratoire de Combustion et de Détonique, UPR 9028 CNRS,
ENSMA, BP 40109, 86961 Futuroscope, France

[2]Inspection des Poudres et Explosifs, 8 boulevard Victor, 00303 Armée, Paris, France

1 Introduction

Heterogeneous solid propellant combustion and radiative heat transfer are of widespread interest in fire safety and particularly in pyrotechnic safety. In the case of accidental propellant fires propagating into a storage block it is necessary to predict the thermal expansion of such a chemical source in order to avoid successive rocket motor blasts and thus to limit human and material damages. Accurate and reliable safety parameters can then be defined to design appropriate storage compartments.

The present study is focused on fires of ammonium perchlorate (AP) - hydroxyl-terminated polybutadiene (HTPB) - aluminium (Al) solid propellant which is one of the most energetic materials and is typically used for rocket motor propulsion. Aluminium solid particles are generally added in order to improve the rocket motor specific impulse, making AP/HTPB flame hotter but more complex. Most of them burn very close to the propellant surface, yielding aluminium oxide Al_2O_3, with a size around 1-2 μm [1]. The aluminium particles left (unburnt Al droplets) can form liquid aggregates on the propellant surface and are entrained through the plume zones where combustion is completed. Their size can vary from 10 μm to 300 μm and strongly depends on the coalescence process [2]. The oxidized products condense in the flame zone to form Al_2O_3 smoke whose growth is characterized by simultaneous coagulation and coalescence [3]. Their radiative properties and their effect on the plume radiation of a rocket motor have been particularly studied for the past twenty years [4]. However few studies have been carried out on aluminized solid propellant fire at 1 atm, mainly due to the extreme flame plume characteristics (high temperatures, flame heterogeneity) which make the experimental measurements difficult [5, 6].

Therefore, the main objective of this work is to perform new experimental tests on aluminized solid propellant combustion at 1 atm for validating a numerical tool that can predict the radiative heat transfer induced by AP/HTPB/Al propellant fires.

2 Experimental methods

Two different setups are designed to make the experimental investigation (Fig.1). All the tests operate with one AP/HTPB/Al-based cube and two propellant compositions (20% and 4% of Aluminium in mass) are tested within the first setup.

(a) Large View Tests (b) Tests within Chimney

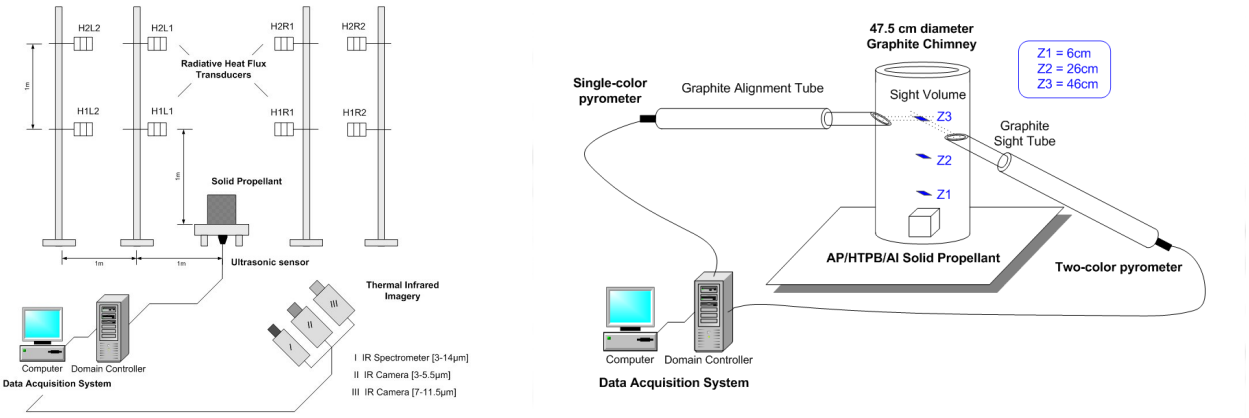

Figure 1: Schemes of the two different experimental setups

Large View Tests

Radiative heat flux is measured by height Medtherm transducers located at 1-2 m distance from the propellant cube and at 1-2 m height from the initial propellant surface. Flame radiance intensity is measured using two AGA782 infrared cameras respectively composed of one near IR band filter [3-5.5 μm] and one far IR band filter [7-11.5 μm]. The emission spectra of the plume is additionally measured by a HGH-SPR314 spectrometer which works between 3 μm and 14 μm with a spectral resolution of $\Delta\lambda$= 1.5%. On the other hand the solid propellant burning rate is measured by an US Panametrics ultrasound sensor which is stuck at the bottom of the sample.

Tests within graphite chimney

In situ flame temperature and local spectral emissivity are measured by pyrometers at three stand-off distances above the initial propellant surface (6 cm, 26 cm and 46 cm). This setup is based on validated experimental techniques [7] and consists in pointing two pyrometers on the same space volume. As aluminized solid propellant flame acts as a graybody between 600 nm and 1200 nm [6], a two-colour IMPAC ISQ 5-LO pyrometer with narrow bandwidths located at 0.90 μm and 1.05 μm is used to infer the true flame temperature. Then, pointing a single-colour pyrometer opposite to the two-colour one and assuming that the test is repeatable, the flame spectral emissivity, at wavelength λ and for the flame temperature T, is deduced from the following relation :

$$\epsilon(\lambda, T) = \exp\left[\frac{C_2}{\lambda}\left(\frac{1}{T} - \frac{1}{T_\lambda}\right)\right]$$

$\epsilon(\lambda$,T) : Flame spectral emissivity
T : Flame Temperature measured by the two-colour pyrometer
T_λ : Radiance temperature at wavelength λ measured by the single colour pyrometer

The single-colour IMPAC ISQ 5-LO pyrometer operates to infer the radiance temperature at λ=0.90 μm while radiance temperatures at λ=4.50 μm and λ=4.66 μm are measured by two single colour Heitronics KT19II pyrometers.

3 Numerical methods

As one of the main objectives of this work is also to simulate aluminized solid propellant fires, computational efforts are simultaneously conducted. Thus, a fire dynamic code which usually computes hydrocarbon fuel combustion, is adapted to aluminized solid propellant fires.

The adiabatic flame temperature and the composition of burnt gases, resulting from AP/HTPB solid propellant combustion at atmospheric pressure, are calculated by a zero-dimensionnal chemical equilibrium based model. As AP/HTPB solid propellant flame height is on the order of hundred microns at 1 atm [8], so very smaller than computational grid cell size (around 1 cm), boundary conditions at the propellant surface are defined to represent the AP/HTPB adiabatic combustion at atmospheric pressure. Burnt gas flow velocity at the propellant surface is calculated from the burning rate measured within the "Large View Tests" and supposed to be uniform on the whole surface.

An approximate form of the Navier-Stokes equations appropriate for low Mach number applications is also computed in the three physical dimensions [9]. This involves the filtering out of acoustic waves while allowing for large variations in temperature and density. The computation is treated as a Large Eddy Simulation (LES) in which the sub-grid scale dissipative processes are modelled [10].

Moreover aluminium droplet dispersion from the burning surface to the plume is taken into account using a lagrangian method. As a result, a force term **f**, a mass term **m** and an energy term **e**, which respectively represent the momentum, mass and energy transferred from the aluminium droplets to the gas, are added to the basic conservation equations. The droplet size distribution is also expressed in terms of its Cumulative Volume Fraction (CVF) and Al droplet oxydation is typically modeled by a d^n droplet combustion law coupled with a mixture fraction model:

$$\begin{cases} \frac{dm_{Al}}{dt} = -\rho_{Al}\frac{\pi}{2}\frac{k}{n}d_{Al}^{3-n} & \text{with n = 2} \\ \\ k = 4ShD_{gas}ln(1+B_m) & \text{B}_m \text{ : Spalding parameter} \end{cases}$$

m_{Al}, ρ_{Al} and d_{Al} are respectively the mass, density and diameter of the Aluminium droplet. Sh is the droplet Sherwood number, given by a correlation involving the Reynolds and Schmidt numbers, and D_{gas} is the gas diffusion coefficient.

Finally the radiative transport equation for a semi-transparent medium is solved by a Finite Volume Method. The model takes into account not only gas radiation but also the absorption and scattering of burning aluminium droplets. Therefore the computed Radiative Transfer Equation is written as :

$$s \cdot \nabla I_\lambda(x,s) = -[\kappa_d(x,\lambda) + \sigma_d(x,\lambda)]I_\lambda(x,s) + \kappa_d(x,\lambda)I_{b,d}(x,\lambda) + \frac{\sigma_d(x,\lambda)}{4\pi}\int_{4\pi}\Phi(s,s')I_\lambda(x,s')d\Omega'$$

where κ_d is the droplet absorption coefficient, σ_d is the droplet scattering coefficient and $I_{b,d}$ is the emission term of the droplets. $\Phi(s,s')$ is a scattering phase function that gives the scattered intensity from direction s' to s. The local absorption and scattering coefficients are calculated from the local number density N(x) and mean diameter d_m(x) as :

$$\begin{cases} \kappa_d(x,\lambda) = N(x)\int_0^\infty f(r,d_m(x))C_a(r,\lambda)dr \\ \\ \sigma_d(x,\lambda) = N(x)\int_0^\infty f(r,d_m(x))C_s(r,\lambda)dr \end{cases}$$

where r is the droplet radius and C_a and C_s are respectively absorption and scattering cross sections given by Mie theory.

4 Main results

(a) Three-cone model [5] (b) Experimental IR view (c) Computed fire plume

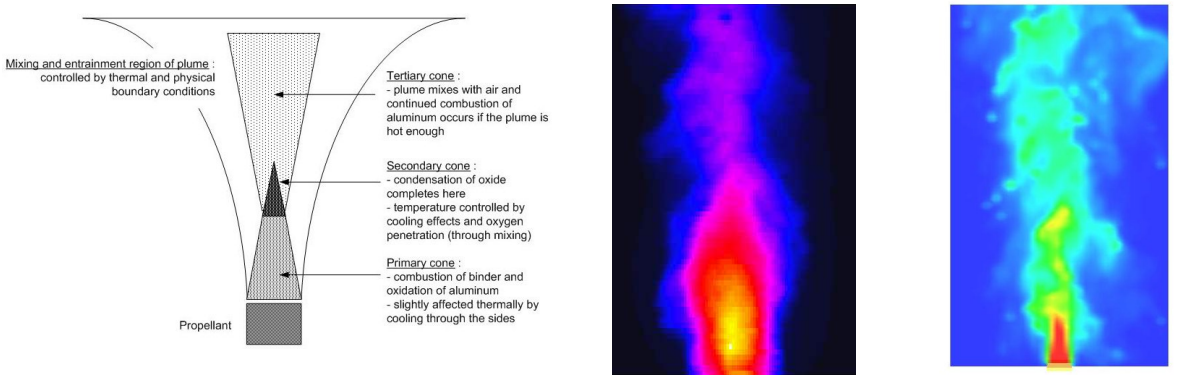

Figure 2: Aluminized solid propellant fire plume

The three-cone structure of the aluminized solid propellant fire plume is pointed out by both experimental and numerical tests (Fig.2). Referencing to the conceptual model depicted by Price [5], three main areas can be observed: - the hottest zone just above the burning propellant surface where gas reactions take place and where Al droplets start burning - the secondary cone where aluminium combustion and condensation of oxide complete - the tertiary cone where flame plume mixes with air and where Al droplet combustion can occur if the plume is hot enough.

(a) (b)

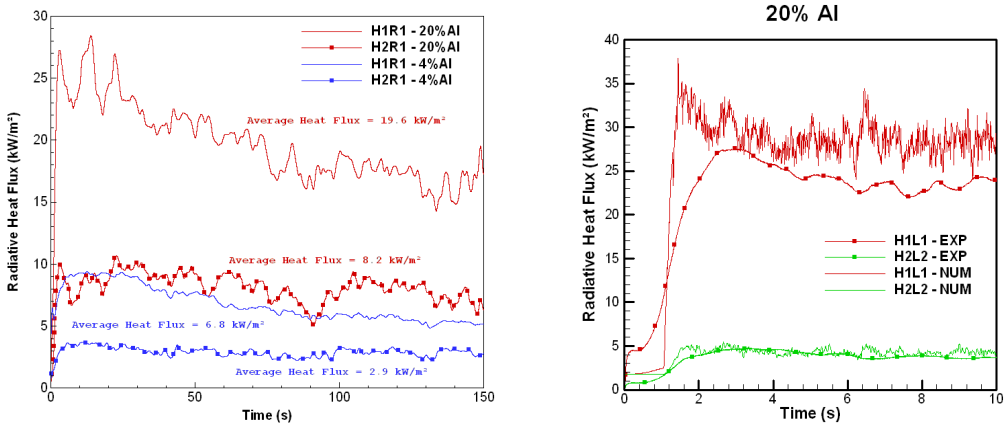

Figure 3: (a) Radiative heat flux from two aluminized solid propellant compositions (20%Al and 4%Al in mass) (b) Numerical prediction of the 20%Al propellant flame plume radiation

On the other hand, radiative heat transfer to the surroundings is pretty much improved with the increasing Al-ratio. Average radiative heat flux is almost three times greater when operating with the 20% Al propellant than with the 4% Al one whatever the captor location (Fig.3a). At 1 m height from the reacting source, flame radiation is mainly induced by burning aluminium droplets. Temperature into this plume area is very high and Al droplet combustion is going on. On the contrary, most of the Al droplet combustion is completed at 2 m height so that flame plume is mainly composed of alumina

particles and agglomerates. Plume temperature falls down due to the mixing with the ambient air and that explains the curving of the heat flux at 2 m height. Similar trends are obtained by numerical calculations (Fig.3b). Radiative heat flux are quite-well predicted, even far away from the burning propellant surface, and the numerical results also show how predominant Al/Al_2O_3 droplets' radiation is on overall radiative heat transfer to the surroundings.

Thus, the radiative emission of aluminized propellant flame seems to be controlled by Al_2O_3 particle radiation. Experimental data of Al_2O_3 emission properties were collected by Sarou Kanian et al. [11] for three alumina solid particle temperatures ($T \leq T_m^{Al_2O_3}$) at the [1.8-9 μm] narrow bandwidth and have been directly compared with the AP/HTPB/20%Al flame emission data. As it was expected, flame spectral emissivity follows up the alumina solid particle one so that it is pretty greater in the mid IR than at around 1 μm.

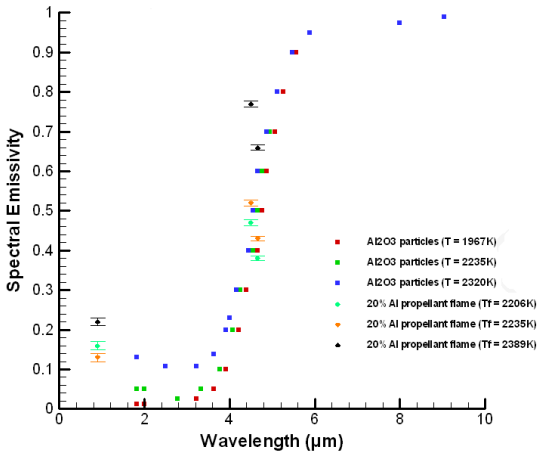

Figure 4: Comparison of spectral emissivity between Al_2O_3 particles and AP/HTPB/20%Al propellant flame in the IR region

5 Conclusion

The main part Al/Al_2O_3 burning droplets play on the radiative heat transfer from aluminized propellant fire plume to the surroundings has been showed by both numerical and experimental tests. For the first time, a numerical model that can predict the thermal environment of Al-based solid propellant combustion at 1 atm is presented. However further developments, particularly on the droplet combustion modeling, could allow to take into account the interaction between turbulence and combustion.

References

[1] G. Lengellé et al. (2000). Physico-Chemical Mechanisms of Solid Propellant Combustion. Progress in Astronautics and Aeronautics (Vol 185), pp 287:334

[2] E.W. Price and R.K. Sigman (2000). Combustion of Aluminized Solid Propellants. Progress in Astronautics and Aeronautics (Vol 185), pp 663:689

[3] V.V. Karasev, A.A. Onishuk, O.G. Glotov, A.M. Baklanov, A.G. Maryasov, V.E. Zarko, V.N. Panfilov, A.I. Levykin, K.K. Sabelfeld (2004). Formation of charged aggregates of Al2O3 nanoparticles by combustion of aluminum droplets in air. Combustion and Flame (138) pp 40:54

[4] D. Laredo, D.W. Netzer (1993). The dominant effect of alumina on nearfield plume radiation. Journal of Quantitative Spectroscopy Radiative Transfer (Vol 50,n°5), pp 511:530

[5] E.W. Price (1979). The fire environment of a solid rocket propellant burning in air. Air Force Weapons Laboratory. Final Report

[6] J.C. Diaz (1993). Thermal environment of a solid rocket propellant fire in ambient atmospheric conditions. JANNAF Combustion Subcommittee Meeting.

[7] R.B. Johnson, C. Feng, and J. Fehribach (1988). On the validity and Techniques of temperature measurement and emissivity measurements. SPIE, Thermosense X (Vol 934), pp 202-206

[8] M.W. Beckstead (2000). Overview of Combustion Mechanisms and Flame Structures for Advanced Solid Propellants. Progress in Astronautics and Aeronautics (Vol 185), pp 267:287

[9] K. Mac Grattan (2004). Fire Dynamics Simulator (V4) Technical Reference Guide (NIST).

[10] J. Smagorinsky (1963). General Circulation experiments with the primitive equations. Monthly weather review (Vol 91, n°3), pp 99-164

[11] V. Sarou-Kanian et al. (2005). IR Radiative Properties of Solid and Liquid Alumina : Effects of temperature and gaseous environment. International Journal of Thermophysics (Vol 26, number 4), pp 1263:1276.